



## INVESTIGATION OF GAMMA-RAY SHIELDING PERFORMANCE OF BOROSILICATE GLASSES DOPED WITH TiO<sub>2</sub> USING PHY-X/PSD AND XCOM SOFTWARE

<sup>1</sup>Huzaifa Saidu Rogo, <sup>\*1,2</sup>Musa, A. and <sup>2</sup>Ibrahim Maijawa

<sup>1</sup>Department of Physics, Bayero University Kano (BUK).

<sup>2</sup>Department of Physics, Federal University Gushua, Yobe State

\*Corresponding Authors email: [amusa.phy@buk.edu.ng](mailto:amusa.phy@buk.edu.ng)

### ABSTRACT

Growing demand for eco-friendly gamma-ray shielding materials has inspired interest in borosilicate glasses enhanced with heavy metal oxides (HMOs). This study uniquely evaluates the influence of borosilicate glasses doped with TiO<sub>2</sub> across a broad energy range Spectrum. The gamma-ray shielding performance of TiO<sub>2</sub>-doped borosilicate glasses with the composition of 30B<sub>2</sub>O<sub>3</sub>–(70-x)SiO<sub>2</sub>–xTiO<sub>2</sub> glass system was investigated (where x = 0, 1, 2, 3, 4 and 5mol%). Shielding parameters mass attenuation coefficient (MAC), half-value layer (HVL), tenth-value layer (TVL), mean free path (MFP), and effective atomic number (Z<sub>eff</sub>) were calculated using the Phy-X/PSD software over photon energies from 0.015 – 15MeV. The mass attenuation coefficient results obtained were cross-verified with XCOM database values, demonstrating close correlation and validating the computational accuracy. The results revealed that increasing TiO<sub>2</sub> concentration led to a slight but consistent enhancement in gamma-ray shielding compared to the undoped sample. GDTi5 exhibited the best performance, with a MAC of 5.400 cm<sup>2</sup>/g, Z<sub>eff</sub> of 13.05, HVL of 0.0497 cm, and MFP of 0.070 cm at 0.015 MeV. The order of shielding effectiveness was GDTi5 > GDTi4 > GDTi3 > GDTi2 > GDTi1 > undoped. These TiO<sub>2</sub>-doped borosilicate glasses, especially GDTi5, are suitable for applications requiring moderate radiation protection and optical transparency, such as diagnostic imaging rooms, nuclear laboratory windows, and portable protective screens.

**Keywords:** TiO<sub>2</sub>-doped borosilicate glass, Gamma-ray shielding, Phy-X/PSD, WinXCom, Mass Attenuation Coefficient (MAC), Radiation protection, Heavy Metal Oxide (HMO)

### INTRODUCTION

In recent years, ionizing radiation has emerged as a significant concern across various industries, including medical imaging, nuclear power, food sterilization, and scientific research (Bagheri *et al.*, 2018; Chai *et al.*, 2020). Prolonged exposure to this type of radiation can have serious health consequences, ranging from radiation sickness and cancer to genetic mutations and even fatal outcomes (Desouky *et al.*, 2015; Stone *et al.*, 2003). Given these risks, effective radiation protection is essential to safeguard human health and minimize exposure. One of the most reliable methods for reducing radiation exposure is the use of shielding materials (Aşkın *et al.*, 2019). The effectiveness of shielding depends on both the type of radiation and the elemental composition of the material (Sayyed *et al.*, 2018).

Shielding materials work by absorbing or scattering photons, thereby reducing their energy and intensity. The best shielding materials typically have high atomic numbers and (Agar *et al.*, 2019; Sayyed *et al.*, 2018). Researchers are increasingly focusing on materials that not only provide strong radiation protection but also possess desirable structural, optical, and thermal properties (Abouhaswa *et al.*, 2021).

Although lead is a common choice for gamma-ray shielding due to its excellent attenuation properties, its toxicity and heavy weight have prompted scientists to explore safer and lighter alternatives, such as polymers, ceramics, concrete, and glass (Baltas *et al.*, 2019). Among these, glass stands out as a particularly promising option because of its affordability, transparency, environmental friendliness, and the ability to incorporate heavy metal oxides like Pb, W, Bi, and Ba. Borate-based glasses, which use boron oxide (B<sub>2</sub>O<sub>3</sub>) as a glass former, are especially valuable due to their high refractive index, low melting point, and versatility (Okada *et al.*, 2025). These glasses are widely used in applications such as laser

systems, solar cells, and gamma-ray detectors (Othman *et al.*, 2021). Their radiation shielding performance can be further enhanced by doping them with heavy metal oxides. This leads to growing interest in modifying borosilicate glass compositions to improve both shielding and fictional properties.

Borosilicate glass, primarily made of SiO<sub>2</sub> and B<sub>2</sub>O<sub>3</sub>, has gained attention as an excellent radiation shielding material due to its thermal and chemical stability, high durability, and low thermal expansion (Chen *et al.*, 2021). Studies have shown that adding metal oxides like BaO can significantly improve shielding efficiency (Kolavekar *et al.*, 2018; Mhareb *et al.*, 2020). Rare earth oxides, such as Nd, Gd, Dy, and La, have also been found to enhance attenuation in glass-ceramics (Mostafa *et al.*, 2022). In particular, gadolinium (Gd) offers notable benefits due to its high atomic number and density (Yonphan *et al.*, 2021). Another promising dopant is titanium dioxide (TiO<sub>2</sub>), which may offer improved attenuation while preserving desirable glass properties.

While the effects of TiO<sub>2</sub> on gamma shielding have been studied at specific photon energies using Geant4, fewer studies have evaluated its performance across a broad energy spectrum. This study addresses that gap by examining TiO<sub>2</sub>-doped borosilicate glasses over a wide range of photon energies of 0.015–15 MeV using the Phy-X/PSD software. The mass attenuation coefficient ( $\mu/\rho$ ) will be validated using XCOM data (Berger & Hubbell, 1987). Key shielding parameters such as the mass attenuation coefficient ( $\mu/\rho$ ), effective atomic number (Z<sub>eff</sub>), half-value layer (HVL), and mean free path (MFP), will be analyzed and compared with reference materials.

### MATERIALS AND METHODS

This study examined the gamma-ray attenuation properties of borosilicate glasses with the composition 30B<sub>2</sub>O<sub>3</sub>–

(70-x)SiO<sub>2</sub>-xTiO<sub>2</sub>, where x ranges from 0 to 5 mol%, across photon energies of 0.015–15 MeV (Al-Hadeethi & Sayyed, 2019). The selected energy spectrum from 0.015–15 MeV covers the lower, medium, and high-energy photons that are typically encountered in nuclear medicine, radiology, and radiation shielding applications. The glass samples included an undoped composition (2.548 g/cm<sup>3</sup>) and five TiO<sub>2</sub>-doped variants: GDTi1 (2.547 g/cm<sup>3</sup>), GDTi2 (2.572 g/cm<sup>3</sup>), GDTi3 (2.594 g/cm<sup>3</sup>), GDTi4 (2.614 g/cm<sup>3</sup>), and GDTi5 (2.634

g/cm<sup>3</sup>). The TiO<sub>2</sub> concentration was limited to 0–5 mol% to maintain glass network stability and ensure homogeneous dispersion of TiO<sub>2</sub> without compromising the physical and optical properties of the host matrix. The complete sample details, including composition, density, and identification codes, are presented in Table 1 (Al-Hadeethi & Sayyed, 2019). Figure 1 demonstrates the progressive increase in glass density with rising TiO<sub>2</sub> concentration.

**Table 1: Samples code, elemental mole fraction and density of 30B<sub>2</sub>O<sub>3</sub>-(70-x)SiO<sub>2</sub>-xTiO<sub>2</sub> glasses**

Sample code	B <sub>2</sub> O <sub>3</sub> (mol%)	SiO <sub>2</sub> (mol%)	Bi <sub>2</sub> O <sub>3</sub> (mol%)	Desity (g/cm <sup>3</sup> )
Undoped	30	70	0	2.548
GDTi1	30	69	1	2.547
GDTi2	30	68	2	2.572
GDTi3	30	67	3	2.594
GDTi4	30	66	4	2.614
GDTi5	30	65	5	2.634

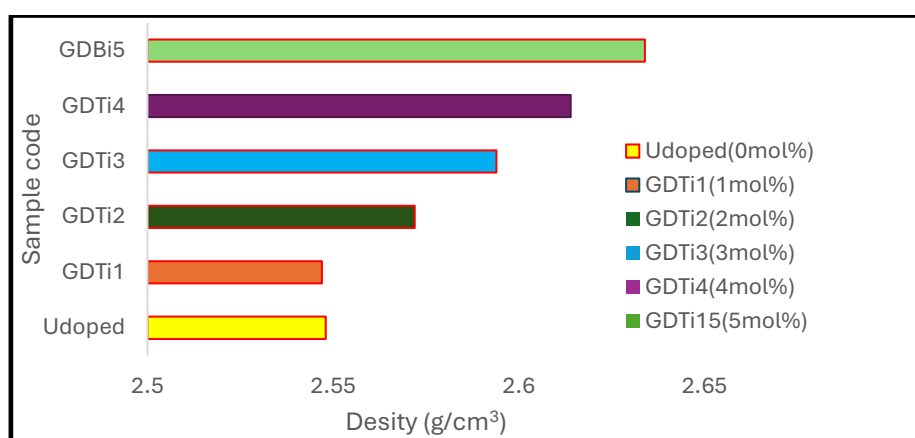


Figure 1: Variation of glass densities (g/cm<sup>3</sup>) as the dopants is gradually increased

**Theoretical Background**

This research focused on evaluating how incorporating titanium oxide (TiO<sub>2</sub>) affects the radiation attenuation capabilities of borosilicate-based glass compositions. To fully understand how photons interact with matter, it’s important to consider the Beer-Lambert law (Mhareb et al., 2020). This equation describes how the intensity of a monoenergetic photon beam decreases as it travels through a material, and is expressed as:

$$I = I_0 e^{-\mu t} \tag{1}$$

Where,  $I_0$  is the intensity of incident photon, and  $I$  is the intensity of the same photon when it passes through absorbing material of thickness  $t$  and linear attenuation coefficient of  $\mu$ . The linear attenuation coefficient (LAC,  $\mu$ ) is a key parameter that helps determine how likely photons are to interact with the glass samples under study (Fakher Alfahed et al., 2019). It is closely related to the mass attenuation coefficient (MAC,  $\mu_m$ ), which reflects the probability of gamma photons interacting with the material per unit mass which is give a can be calculated with the relation (Mostafa et al., 2022).

$$\mu_m = \left[ \frac{\mu}{\rho} \right] = \frac{\ln(I_0/I)}{\rho t} = \frac{\ln(I_0/I)}{t_m} \tag{2}$$

Where  $\mu$  (cm<sup>-1</sup>) and  $\mu_m$  (cm<sup>2</sup>/g) are linear and mass attenuation coefficients,  $t$  (cm) and  $t_m$  (g/cm<sup>2</sup>) are the thickness and sample mass thickness (the mass per unit area), and  $\rho$  (g/cm<sup>3</sup>) is the density of material. Other key parameters used to evaluate the required thickness of shielding materials include the half-value layer (HVL) and tenth-value layer (TVL). These parameters are essential for understanding how well a material can reduce radiation intensity.

The HVL represents the thickness of a material needed to reduce the intensity of gamma radiation by 50%. In this study, HVL will be used to assess the ability of the glass samples to attenuate gamma rays at various energies. This parameter can be calculated by dividing the natural logarithm of 2 by the linear attenuation coefficient, as expressed below (Jamal et al., 2020).

$$HVL = \frac{\ln 2}{\mu} = \frac{0.693}{\mu} \tag{3}$$

Similarly, tenth-value layer (TVL) refers to the thickness required to reduce the incident gamma-ray intensity to one-tenth of its original value. The TVL is calculated using the following relation (Jamal et al., 2020).

$$TVL = \frac{\ln(10)}{\mu} \tag{4}$$

The mean free path (MFP) is an important parameter that helps describe how photons behave as they pass through glass. It indicates the average distance a photon can travel in the material before being scattered or absorbed. A shorter MFP means the material is more effective at stopping radiation. It is inversely related to the linear attenuation coefficient (LAC) and the MFP can be evaluated from  $\mu$  (cm<sup>-1</sup>) using the relation below (Basha et al., 2023).

$$MFP = \frac{\int_0^\infty t e^{-\mu t} dt}{\int_0^\infty e^{-\mu t} dt} = \frac{1}{\mu} \tag{5}$$

The total atomic cross-sections ( $\delta_a$ ; cm<sup>2</sup>/g) for any sample can be calculated from the mass attenuation coefficients utilizing the next equation:

$$\delta_a = \frac{N \mu_m}{N_A} \tag{6}$$

Where  $N_A$  is Avogadro constant. And the total electronic cross-sections ( $\delta_a$ ;  $\text{cm}^2/\text{g}$ ) is given by the following formula (Han & Demir, 2009):

$$\delta_l = \frac{1}{N_A} \left[ \frac{f_i A_i}{Z_i} (\mu_m)_i \right] = \frac{\delta_a}{Z_{eff}} \tag{7}$$

Where  $Z_i$ ,  $f_i$ ,  $(\mu_m)$  and  $A_i$  are the atomic number, mole fraction, mass attenuation coefficient and atomic weight of the  $i$ th constituent element, respectively. The effective atomic number ( $Z_{eff}$ ) is a parameter that represents the overall effective atomic number of a multi-element material, like glass, when interacting with ionizing radiation. It combines the contributions of all elements in the material, providing a measure of its ability to attenuate or absorb radiation, particularly gamma rays. From the parameters given in equation (6) and equation (7), we can evaluate  $Z_{eff}$  using the next relation (Aşkın *et al.*, 2019).

$$Z_{eff} = \frac{\delta_a}{\delta_l} \tag{8}$$

These parameters were computed using the following well-established equations by utilizing the Phy-X/PSD software (Şakar *et al.*, 2020)

**RESULTS AND DISCUSSION**

The Mass Attenuation Coefficient (MAC) is a key shielding parameter that defines how effectively a material can attenuate incoming gamma rays. In this study, MAC values were evaluated for the selected borosilicate glass samples Undoped, GDTi1, GDTi2, GDTi3, GDTi4, and GDTi5 using the Phy-X/PSD software across a wide photon energy range of 15 keV to 15 MeV, considering Cobalt-60 and Cesium-137 as gamma sources. To ensure accuracy, the MAC values obtained for both the undoped and  $\text{TiO}_2$ -doped glasses with varying molar concentrations of 1-5mol% were validated using the XCOM software, and the results are summarized and presented in Table 2. A strong agreement was observed between the values from Phy-X/PSD and XCOM, reinforcing the reliability of the results. However, minor discrepancies were observed between the MAC values obtained from Phy-X/PSD and XCOM, particularly at certain energy levels. For instance, at 0.030 MeV, the MAC value for the GDTi1 sample was 0.734  $\text{cm}^2/\text{g}$  using Phy-X/PSD and 0.736  $\text{cm}^2/\text{g}$  using XCOM. Similarly, at 0.600 MeV, a slight deviation of 0.001  $\text{cm}^2/\text{g}$  was noted for the same sample. These variations are

minimal and can be attributed to differences in computational algorithms, rounding approaches, or the underlying theoretical models employed by each software. Such differences are within acceptable limits and do not significantly impact the overall accuracy or interpretation of the results. The plot of the mass attenuation coefficient (MAC) for the undoped and  $\text{TiO}_2$ -doped borosilicate glasses are illustrated in Figure 2, and for comparison, the plot also includes the undoped sample to highlight the impact of heavy metal oxide addition on the attenuation performance of the glasses. It's important to note that glasses with higher MAC values are more effective at shielding against incoming photons compared to those with lower values. As shown in Table 2, increasing the  $\text{TiO}_2$  content from 1 mol% to 5 mol% resulted in a slight increase in the Mass Attenuation Coefficient. As illustrated in Figure 2, the mass attenuation coefficient (MAC) shows a clear decreasing trend as the photon energy increases from 15 keV to 15 MeV. This observation confirms that higher gamma-ray energies tend to reduce the MAC values, thereby lowering the interaction probability between photons and glass materials. The maximum MAC values for all the investigated samples were observed at 15 keV. Specifically, the MAC was 4.351  $\text{cm}^2/\text{g}$  for the undoped sample, 4.701  $\text{cm}^2/\text{g}$  for GDTi1, 4.775  $\text{cm}^2/\text{g}$  for GDTi2, 4.984  $\text{cm}^2/\text{g}$  for GDTi3, 4.193  $\text{cm}^2/\text{g}$  for GDTi4, and 5.400  $\text{cm}^2/\text{g}$  for GDTi5. However, it was observed that the GDTi5 sample exhibits a slightly higher MAC compared to the remaining samples. This is primarily because GDTi5 has the highest density among all the investigated glasses, which indicates a partial enhancement in the attenuation capability of the borosilicate glass system used in this study. These high MAC values at low energy (15 keV) are primarily attributed to the photoelectric effect, which dominates in this energy range. This interaction is highly dependent on the atomic number ( $Z^{4-5}$ ) of the elements present in the glass composition, as highlighted by Şakar *et al.* (2020). Furthermore, as shown in Figure 2, the mass attenuation coefficient (MAC) values for the glass samples remain relatively constant across the energy range of 0.100 to 15 MeV. This trend is attributed to the dominance of Compton scattering in this energy region. The likelihood of Compton scattering occurring tends to increase linearly with atomic number ( $Z$ ), as explained by Agar *et al.* (2019).

**Table 2: The Mass Attenuation Coefficient ( $\text{cm}^2/\text{g}$ ) of Undoped and Titanium Oxide Doped Borosilicate Glass obtained through Phy-X/PSD and XCOM**

Photon energy (MeV)	Undoped		GDTi1		GDTi2		GDTi3		GDTi4		GDTi5	
	Phy-X	Xcom	Phy-X	Xcom	Phy-X	Xcom	Phy-X	Xcom	Phy-X	Xcom	Phy-X	Xcom
0.015	4.351	4.350	4.701	4.700	4.775	4.770	4.984	4.989	5.193	5.189	5.400	
0.020	1.931	1.931	2.073	2.073	2.119	2.117	2.212	2.214	2.305	2.303	2.396	
0.030	0.691	0.691	0.734	0.736	0.749	0.748	0.778	0.778	0.806	0.808	0.835	
0.040	0.389	0.389	0.410	0.409	0.413	0.413	0.426	0.426	0.438	0.438	0.450	
0.050	0.279	0.279	0.225	0.220	0.291	0.291	0.298	0.298	0.304	0.304	0.310	
0.060	0.228	0.228	0.220	0.219	0.235	0.235	0.239	0.239	0.243	0.242	0.246	
0.080	0.183	0.183	0.170	0.169	0.186	0.186	0.187	0.187	0.189	0.189	0.190	
0.100	0.162	0.162	0.163	0.163	0.164	0.164	0.165	0.165	0.165	0.165	0.166	
0.150	0.138	0.138	0.138	0.138	0.138	0.138	0.138	0.138	0.138	0.138	0.138	
0.200	0.124	0.124	0.124	0.124	0.124	0.124	0.124	0.124	0.124	0.124	0.124	
0.300	0.106	0.107	0.106	0.106	0.106	0.106	0.106	0.106	0.106	0.106	0.106	
0.400	0.095	0.095	0.094	0.094	0.095	0.095	0.095	0.095	0.095	0.095	0.095	
0.500	0.087	0.087	0.085	0.085	0.087	0.087	0.087	0.087	0.087	0.087	0.086	
0.600	0.080	0.080	0.078	0.079	0.080	0.080	0.080	0.080	0.080	0.080	0.080	
0.800	0.070	0.070	0.069	0.069	0.070	0.070	0.070	0.070	0.070	0.070	0.070	

1.000	0.063	0.063	0.062	0.062	0.063	0.063	0.063	0.062	0.063	0.063	0.063
1.500	0.051	0.051	0.050	0.050	0.051	0.051	0.051	0.051	0.051	0.051	0.051
2.000	0.044	0.044	0.043	0.044	0.044	0.044	0.044	0.044	0.044	0.044	0.044
3.000	0.036	0.036	0.036	0.036	0.036	0.036	0.036	0.036	0.036	0.036	0.036
4.000	0.031	0.031	0.031	0.031	0.031	0.031	0.031	0.031	0.031	0.031	0.031
5.000	0.028	0.028	0.029	0.029	0.028	0.028	0.028	0.028	0.028	0.028	0.028
6.000	0.026	0.026	0.027	0.027	0.026	0.026	0.026	0.026	0.026	0.026	0.026
8.000	0.023	0.023	0.025	0.025	0.023	0.024	0.023	0.023	0.023	0.024	0.023
10.00	0.022	0.022	0.024	0.023	0.022	0.022	0.022	0.022	0.022	0.022	0.022
15.00	0.020	0.020	0.023	0.022	0.020	0.020	0.020	0.020	0.020	0.020	0.020

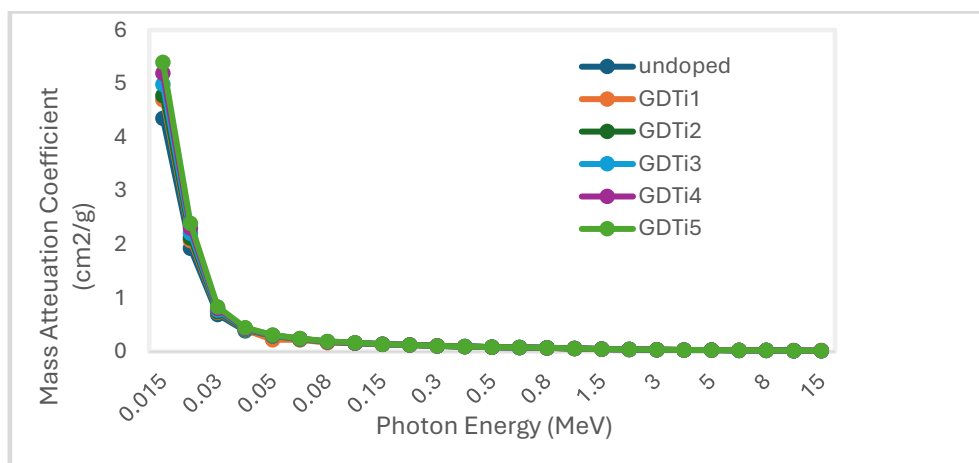


Figure 2: The mass attenuation coefficient of borosilicate glass doped with TiO<sub>2</sub> across Photon energy

As illustrated in Figure 2, it is evident that the glass samples doped with TiO<sub>2</sub> show only slight changes in the mass attenuation coefficient with increasing TiO<sub>2</sub> content. However, these doped samples consistently exhibit higher MAC values compared to the undoped glass. From Figures 2, it can be concluded that the addition of TiO<sub>2</sub> enhances the shielding performance of the borosilicate glasses. The evaluation indicates that GDTi5 demonstrates the highest attenuation capability, followed by GDTi4, GDTi3, GDTi2, GDTi1, and finally the undoped sample. Among all the evaluated glasses, GDTi5 stands out as the most effective attenuator.

The effective atomic number ( $Z_{eff}$ ) is a crucial parameter for evaluating the radiation shielding performance of glass materials. It reflects the combined atomic number of all the elements in a composite material and plays a significant role in determining how well the material can attenuate incoming photons by reducing their number and energy. In general, a higher  $Z_{eff}$  value indicates a stronger ability to block or absorb radiation. In this study, the  $Z_{eff}$  values for both undoped and TiO<sub>2</sub>-doped glasses were calculated using the Phy-X/PSD

software and were well tabulated in Table 3, following the method outlined by Alomari & Al-Qahtani, (2024). Table 3, illustrate how the effective atomic number ( $Z_{eff}$ ) varies with photon energy for the selected borosilicate glasses doped with TiO<sub>2</sub>. From Table 3, it's evident that within the low-energy range of 0.015–0.04 MeV, all the glass samples display high and relatively constant  $Z_{eff}$  values, suggesting that there is minimal dependence on energy in this region. In the intermediate energy range of 0.04–1 MeV, the effective atomic number ( $Z_{eff}$ ) of all glass samples decreases significantly with increasing photon energy. This behaviour is attributed to the dominance of the photoelectric effect in this region. Between 1 - 3 MeV, the  $Z_{eff}$  values remain relatively constant and minimal, which corresponds to the prevalence of Compton scattering, where interaction probability is influenced more by electron density than atomic number. At higher photon energies of 3–15 MeV, a gradual increase in  $Z_{eff}$  is observed, primarily due to the emergence of pair production, which becomes more prominent at higher energies and is highly dependent on the atomic number of the absorbing material.

Table 3: The Effective Atomic Number ( $Z_{eff}$ ) of Borosilicate Glass Doped with Titanium Oxide (TiO<sub>2</sub>) obtained through Phy-X/PSD

Photon energy (MeV)	Effective Atomic Number ( $Z_{eff}$ )					
	Undoped	GDTi1	GDTi2	GDTi3	GDTi4	GDTi5
0.015	11.61	11.93	12.23	12.52	12.79	13.05
0.020	11.42	11.74	12.04	12.32	12.60	12.86
0.030	10.81	11.08	11.34	11.60	11.84	12.07
0.040	10.16	10.38	10.58	10.78	10.98	11.17
0.050	9.68	9.84	9.99	10.14	10.29	10.44
0.060	9.36	9.48	9.59	9.71	9.82	9.93
0.080	9.02	9.09	9.17	9.24	9.31	9.38
0.100	8.87	8.92	8.97	9.02	9.08	9.13

0.150	8.74	8.78	8.81	8.84	8.87	8.91
0.200	8.71	8.73	8.76	8.79	8.82	8.84
0.300	8.68	8.71	8.73	8.76	8.78	8.80
0.400	8.68	8.70	8.72	8.75	8.77	8.79
0.500	8.67	8.70	8.72	8.74	8.76	8.79
0.600	8.67	8.69	8.72	8.74	8.76	8.78
0.800	8.67	8.69	8.71	8.74	8.76	8.78
1.000	8.67	8.69	8.71	8.74	8.76	8.78
1.500	8.67	8.69	8.71	8.74	8.76	8.78
2.000	8.68	8.70	8.72	8.75	8.77	8.79
3.000	8.70	8.73	8.75	8.77	8.80	8.82
4.000	8.73	8.76	8.78	8.81	8.83	8.86
5.000	8.76	8.79	8.82	8.84	8.87	8.90
6.000	8.79	8.82	8.85	8.88	8.91	8.94
8.000	8.85	8.88	8.92	8.95	8.98	9.01
10.00	8.91	8.94	8.98	9.01	9.04	9.08
15.00	9.01	9.05	9.09	9.13	9.17	9.21

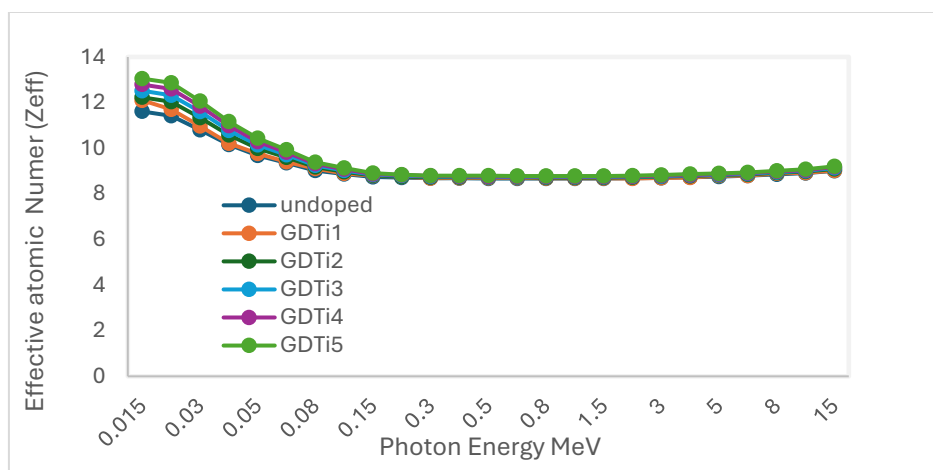


Figure 3: The Variation of Z<sub>eff</sub> with Photon energy of borosilicate glass doped with TiO<sub>2</sub>

From Figure 3, it is clear that the highest Z<sub>eff</sub> values for the TiO<sub>2</sub>-doped samples are observed at 0.015 MeV. As depicted in Figure 3, increasing the TiO<sub>2</sub> concentration from 1 to 5 mol% results in a slight, almost negligible increase in Z<sub>eff</sub>. This is expected, given the similar atomic numbers of silicon (Z = 14) and titanium (Z = 22). At 0.015 MeV, the Z<sub>eff</sub> value for the undoped sample is 11.61, while it increases progressively to 12.10 for GDTi1, 12.23 for GDTi2, 12.52 for GDTi3, 12.59 for GDTi4, and 13.05 for GDTi5. This trend indicates that GDTi5 exhibits the highest Z<sub>eff</sub>, suggesting it offers superior radiation shielding performance, likely due to its higher molecular weight and density.

The penetration ability of gamma photons through glass can be assessed using the Half Value Layer (HVL), which indicates the thickness of material required to reduce the intensity of gamma radiation by 50%. HVL is typically measured in centimetres (cm) or millimetres (mm) and is inversely proportional to the linear attenuation coefficient (μ). Generally, glasses with higher atomic number and density possess greater attenuation capability, resulting in lower HVL values. Therefore, a smaller HVL suggests better shielding performance. In this study, HVL values were evaluated for borosilicate glasses doped with varying concentrations of

TiO<sub>2</sub> to determine their effectiveness in radiation shielding through Phy-X/PSD software, as presented in Table 4. From Table 4, it is evident that as photon energy increases, the HVL values show an upward trend. This is primarily due to the reduced probability of photon interactions at higher energy levels. The lowest HVL among the investigated samples was observed at the lowest energy point of 0.015 MeV. Table 4, shows that the addition of TiO<sub>2</sub> resulted in a slight reduction in HVL for all glass samples. At 0.015 MeV, the undoped sample had an HVL of 0.063 cm, which decreased to 0.060 cm for GDTi1, 0.056 cm for GDTi2, 0.054 cm for GDTi3, 0.051 cm for GDTi4, and 0.049 cm for GDTi5, indicating improved shielding efficiency with increased TiO<sub>2</sub> content. From Table 4, it is evident that the glass sample GDTi5 exhibits the lowest HVL value, followed by GDTi4, GDTi3, GDTi2, GDTi1, and the undoped sample. This clearly indicates that the incorporation of TiO<sub>2</sub> into the borosilicate glass matrix enhances photon attenuation, with GDTi5 having the highest mol% of TiO<sub>2</sub> demonstrating the most effective shielding performance. A similar trend was observed for the Tenth Value Layer (TVL) across all the samples, reaffirming the improved radiation attenuation capability with increasing TiO<sub>2</sub> concentration.

**Table 4: The Half Value Layer (cm) of Borosilicate Glass Doped with Titanium Oxide obtained through Phy-X/PSD**

Photon energy (MeV)	Half Value Layer (HVL)					
	undoped	GDTi1	GDTi2	GDTi3	GDTi4	GDTi5
0.015	0.063	0.060	0.056	0.054	0.051	0.049
0.020	0.141	0.139	0.127	0.121	0.115	0.110
0.030	0.394	0.380	0.360	0.344	0.329	0.315
0.040	0.700	0.656	0.652	0.628	0.606	0.585
0.050	0.976	0.936	0.925	0.897	0.872	0.848
0.060	1.193	1.157	1.145	1.118	1.093	1.069
0.080	1.487	1.480	1.450	1.426	1.404	1.383
0.100	1.676	1.650	1.645	1.624	1.604	1.585
0.150	1.977	1.962	1.953	1.934	1.917	1.900
0.200	2.196	2.188	2.175	2.155	2.138	2.121
0.300	2.555	2.544	2.532	2.511	2.492	2.474
0.400	2.862	2.850	2.837	2.814	2.794	2.774
0.500	3.139	3.124	3.112	3.087	3.065	3.043
0.600	3.396	3.353	3.368	3.341	3.317	3.294
0.800	3.870	3.850	3.838	3.807	3.780	3.753
1.000	4.305	4.300	4.270	4.236	4.206	4.176
1.500	5.288	5.222	5.245	5.203	5.166	5.129
2.000	6.141	6.133	6.089	6.041	5.997	5.955
3.000	7.578	7.562	7.511	7.449	7.394	7.340
4.000	8.739	8.684	8.659	8.585	8.520	8.456
5.000	9.696	9.487	9.602	9.518	9.443	9.369
6.000	10.485	10.470	10.377	10.284	10.201	10.119
8.000	11.688	11.661	11.558	11.449	11.351	11.255
10.00	12.531	12.477	12.381	12.259	12.150	12.042
15.00	13.743	13.636	13.556	13.413	13.282	13.154

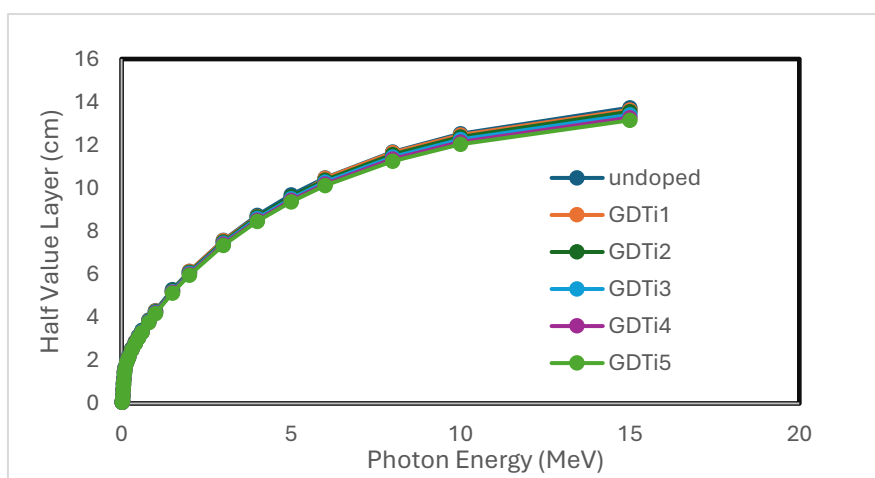


Figure 4: The Variation of HVL with Photon energy of borosilicate glass doped with TiO<sub>2</sub>

From Figure 4, we can clearly see that the GDTi5 glass sample has the lowest HVL value, followed by GDTi4, GDTi3, GDTi2, GDTi1, and finally the undoped glass. This pattern shows that adding TiO<sub>2</sub> to borosilicate glass improves its ability to attenuate photons. Among all, GDTi5 with the highest mol% of TiO<sub>2</sub> stands out as the most effective in enhancing radiation shielding. A similar pattern was also observed for the Tenth Value Layer (TVL) which refers to the thickness of material that reduces the initial intensity by 10%, confirming that higher TiO<sub>2</sub> concentration leads to better shielding performance.

The Mean Free Path (MFP) refers to the average distance a photon or any ionizing particle like gamma rays or neutrons can travel through a material before interacting with it. A lower MFP value indicates that the material is more effective at attenuating radiation. In this study, we assessed the influence of TiO<sub>2</sub> on the gamma-ray shielding ability of borosilicate glass by analysing the MFP values across a photon energy range of 15 keV to 15 MeV, as presented in Table 5.

**Table 5: The Mean Free Path (cm) of Borosilicate Glass Doped with Titanium Oxide obtained through Phy-X/PSD**

Photon energy (MeV)	Mean Free Path (MFP)					
	Undoped	GDTi1	GDTi2	GDTi3	GDTi4	GDTi5
0.015	0.090	0.088	0.081	0.077	0.074	0.070
0.020	0.203	0.200	0.183	0.174	0.166	0.158
0.030	0.568	0.553	0.519	0.496	0.474	0.455
0.040	1.010	1.069	0.941	0.906	0.874	0.844
0.050	1.408	1.628	1.334	1.295	1.258	1.224
0.060	1.722	1.719	1.652	1.614	1.578	1.543
0.080	2.146	2.100	2.092	2.057	2.026	1.995
0.100	2.417	2.399	2.373	2.343	2.315	2.287
0.150	2.852	2.857	2.818	2.791	2.766	2.742
0.200	3.169	3.159	3.137	3.110	3.085	3.060
0.300	3.686	3.680	3.653	3.623	3.596	3.569
0.400	4.129	4.100	4.093	4.060	4.031	4.002
0.500	4.528	4.500	4.490	4.454	4.422	4.390
0.600	4.900	4.890	4.859	4.820	4.786	4.752
0.800	5.583	5.500	5.536	5.492	5.453	5.415
1.000	6.211	6.200	6.160	6.111	6.067	6.025
1.500	7.629	7.600	7.566	7.506	7.453	7.400
2.000	8.859	8.840	8.785	8.715	8.652	8.591
3.000	10.932	10.900	10.836	10.747	10.668	10.590
4.000	12.608	12.529	12.492	12.386	12.292	12.199
5.000	13.989	13.968	13.852	13.732	13.624	13.517
6.000	15.126	15.080	14.971	14.837	14.717	14.599
8.000	16.863	16.714	16.674	16.518	16.376	16.237
10.00	18.078	18.058	17.862	17.687	17.528	17.372
15.00	19.827	19.664	19.558	19.351	19.162	18.977

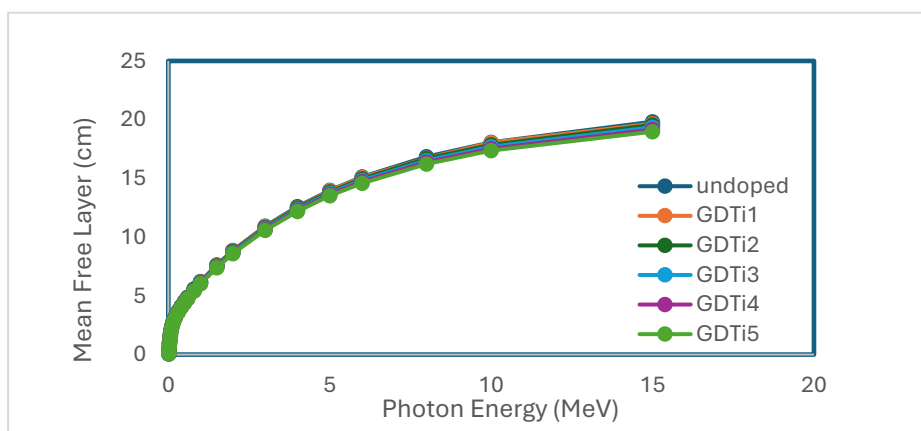


Figure 5: The Variation of MFP with Photon energy of borosilicate glass doped with TiO<sub>2</sub>

Table 5, illustrate how the Mean Free Path (MFP) varies with photon energy for borosilicate glasses doped with TiO<sub>2</sub>. As the photon energy increases, the MFP also increases, indicating that photons are able to travel further through the glass, making penetration easier at higher energies. From Table 5, it's evident that adding TiO<sub>2</sub> leads to only a slight reduction in MFP. For example, at 0.015 MeV, the MFP for the undoped glass is 0.090 cm. With the introduction of TiO<sub>2</sub>, it slightly drops to 0.088 cm in GDTi1, 0.081 cm in GDTi2, 0.077 cm in GDTi3, 0.074 cm in GDTi4, and reaches 0.070 cm in GDTi5. This subtle decline suggests that increased TiO<sub>2</sub> concentration marginally enhances the material's photon attenuation capability. This slight but consistent decrease in MFP with increasing TiO<sub>2</sub> content may be attributed to the trade-off between the moderate atomic number of Ti (Z = 22) and the resulting increase in glass density. Although the

addition of TiO<sub>2</sub> does not significantly elevate the atomic number of the overall composition, the densification effect due to TiO<sub>2</sub> incorporation contributes to improved photon attenuation. Additionally, the results show that the GDTi5 glass sample has the lowest MFP value among all the samples, indicating that GDTi5 is the most effective in absorbing incoming photons. From Figure 5, it's clear that the shielding capabilities of the samples follow this order: GDTi5 > GDTi4 > GDTi3 > GDTi2 > GDTi1 > undoped. This suggests that the addition of HMO to the glass system enhances its shielding performance. Notably, the MFP values of 0.070cm for the GDTi5 glasses are even lower than those of ordinary concrete, as reported by Aşkın et al. (2019), similarly, According to Ummah, (2019), concrete made with 15 mm granite aggregates showed superior gamma-ray attenuation, making it a promising low-cost shielding material for

unregulated radiation facilities in Nigeria, underscoring its potential for practical applications. This trend suggests that GDTi5 may be suitable for compact radiation shielding designs, especially in settings with spatial constraints such as medical diagnostic rooms or aerospace components, where lightweight and effective materials are essential.

## CONCLUSION

This research studied the radiation shielding performance of borosilicate glasses doped with different amounts of titanium dioxide ( $\text{TiO}_2$ ) in the composition  $30\text{B}_2\text{O}_3-(70-x)\text{SiO}_2-x\text{TiO}_2$ , where  $x = 0, 1, 2, 3, 4$ , and  $5$  mol%. Using Phy-X/PSD software, we calculated important shielding parameters such as Mass Attenuation Coefficient (MAC), Half-Value Layer (HVL), Tenth-Value Layer (TVL), Mean Free Path (MFP), and Effective Atomic Number ( $Z_{\text{eff}}$ ), across a wide energy range (0.015 to 15 MeV). The MAC results were also confirmed using the XCOM database, showing strong agreement.

The results showed that adding  $\text{TiO}_2$  slightly but steadily improved the shielding ability of the glass compared to the undoped sample. Among all the glass samples, GDTi5 which contain 5 mol% of  $\text{TiO}_2$  exhibited the best performance, with the highest attenuation and the lowest penetration metrics across the studied energies. This means GDTi5 is the most effective at blocking gamma rays. The overall order of shielding performance was:  $\text{GDTi5} > \text{GDTi4} > \text{GDTi3} > \text{GDTi2} > \text{GDTi1} > \text{undoped}$ .

Finally,  $\text{TiO}_2$ -doped borosilicate glasses, especially GDTi5, are promising materials for radiation shielding. They offer good protection while remaining transparent, making them useful for medical imaging rooms, nuclear lab windows, and portable protective screens. Future studies could explore higher  $\text{TiO}_2$  concentrations or investigate hybrid dopants to further enhance shielding properties and tailor the glasses for specific applications.

## REFERENCES

- Abouhaswa, A. S., Zakaly, H. M. H., Issa, S. A. M., Rashad, M., Pyshkina, M., Tekin, H. O., El-Mallawany, R., & Mostafa, M. Y. A. (2021). Synthesis, physical, optical, mechanical, and radiation attenuation properties of  $\text{TiO}_2$ - $\text{Na}_2\text{O}$ - $\text{Bi}_2\text{O}_3$ - $\text{B}_2\text{O}_3$  glasses. *Ceramics International*, 47(1), 185–204. <https://doi.org/10.1016/j.ceramint.2020.08.122>
- Agar, O., Khattari, Z. Y., Sayyed, M. I., Tekin, H. O., Al-Omari, S., Maghrabi, M., Zaid, M. H. M., & Kityk, I. V. (2019). Evaluation of the shielding parameters of alkaline earth based phosphate glasses using MCNPX code. *Results in Physics*, 12(November 2018), 101–106. <https://doi.org/10.1016/j.rinp.2018.11.054>
- Al-Hadeethi, Y., & Sayyed, M. I. (2019). Analysis of borosilicate glasses doped with heavy metal oxides for gamma radiation shielding application using Geant4 simulation code. *Ceramics International*, 45(18), 24858–24864. <https://doi.org/10.1016/j.ceramint.2019.08.234>
- Alomari, A. H., & Al-Qahtani, S. M. (2024). Enhanced gamma shielding properties of borosilicate glasses with  $\text{Gd}_2\text{O}_3$  addition: A theoretical study using Phy-X/PSD and XCOM programs. *Journal of Radiation Research and Applied Sciences*, 17(3), 100996. <https://doi.org/10.1016/j.jrras.2024.100996>
- Aşkın, A., Sayyed, M. I., Sharma, A., Dal, M., El-Mallawany, R., & Kaçal, M. R. (2019). Investigation of the gamma ray

shielding parameters of  $(100-x)[0.5\text{Li}_2\text{O}-0.1\text{B}_2\text{O}_3-0.4\text{P}_2\text{O}_5]-x\text{TeO}_2$  glasses using Geant4 and FLUKA codes. *Journal of Non-Crystalline Solids*, 521(May). <https://doi.org/10.1016/j.jnoncrysol.2019.119489>

Bagheri, R., Moghaddam, A. K., Shirmardi, S. P., Azadbakht, B., & Salehi, M. (2018). Determination of gamma-ray shielding properties for silicate glasses containing  $\text{Bi}_2\text{O}_3$ ,  $\text{PbO}$ , and  $\text{BaO}$ . *Journal of Non-Crystalline Solids*, 479(October), 62–71. <https://doi.org/10.1016/j.jnoncrysol.2017.10.006>

Baltas, H., Sirin, M., Celik, A., Ustabas, & El-Khayatt, A. M. (2019). Radiation shielding properties of mortars with minerals and ores additives. *Cement and Concrete Composites*, 97(January), 268–278. <https://doi.org/10.1016/j.cemconcomp.2019.01.006>

Basha, B., Alsufyani, S. J., Olarinoye, I. O., Alrowaili, Z. A., Sadeq, M. S., Misbah, M. H., Rammah, Y. S., Abouhaswa, A. S., & Al-Buriahi, M. S. (2023). Synthesis, physical, optical, and radiation attenuation efficiency of  $\text{Bi}_2\text{O}_3$ - $\text{SrF}_2$ - $\text{Li}_2\text{O}$  glass system. *Journal of Radiation Research and Applied Sciences*, 16(4), 100676. <https://doi.org/10.1016/j.jrras.2023.100676>

Berger, M., & Hubbell, J. H. (1987). XCOM: Photon cross sections on a personal computer. *National Bureau of Standards, Washington, DC (USA). Center for Radiation Research*, 1–28. <http://www.pma.caltech.edu/~dons/ph3-7/wave/phapps/xcom/xcom.doc>

Chai, F., Wang, G., Liu, F., Jiang, D., Yao, C., Xu, T., & Dai, Y. (2020). Preparation and properties of flame-retardant neutron shielding material based on EVA polymer reinforced by radiation modification. *Radiation Physics and Chemistry*, 174(April), 108984. <https://doi.org/10.1016/j.radphyschem.2020.108984>

Chen, L. T., Mao, J. J., Mao, Y. N., Zhang, X. Y., Sun, M. L., Wang, T. T., Wang, T. S., & Peng, H. B. (2021). Changes in macroscopic and microscopic properties of borosilicate glass irradiated with ions. *Radiation Effects and Defects in Solids*, 176(9–10), 789–803. <https://doi.org/10.1080/10420150.2021.1955253>

Desouky, O., Ding, N., & Zhou, G. (2015). Targeted and non-targeted effects of ionizing radiation. *Journal of Radiation Research and Applied Sciences*, 8(2), 247–254. <https://doi.org/10.1016/j.jrras.2015.03.003>

Fakher Alfahed, R. K., Mohammad, K. K., Majeed, M. S., Ali Badran, H., Ali, K. M., & Yahya Kadem, B. (2019). Preparation, morphological, and mechanical characterization of titanium dioxide ( $\text{TiO}_2$ )/polyvinyl alcohol (PVA) composite for gamma-rays radiation shielding. *Journal of Physics: Conference Series*, 1279(1). <https://doi.org/10.1088/1742-6596/1279/1/012019>

Jamal, N., Natasha, M., Aida, N., & Amin, B. (2020). Tungsten-based material as promising new lead-free gamma radiation shielding material in nuclear medicine. *Physica Medica*, 78(July), 48–57. <https://doi.org/10.1016/j.ejmp.2020.08.017>

Kolavekar, S. B., Ayachit, N. H., Jagannath, G., NagaKrishnakanth, K., & Venugopal Rao, S. (2018). Optical,

- structural and Near-IR NLO properties of gold nanoparticles doped sodium zinc borate glasses. *Optical Materials*, 83(May), 34–42. <https://doi.org/10.1016/j.optmat.2018.05.083>
- Mhareb, M. H. A., Alajerami, Y. S. M., Sayyed, M. I., Dwaikat, N., Alqahtani, M., Alshahri, F., Saleh, N., Alonizan, N., Ghrib, T., & Al-Dhafar, S. I. (2020). Radiation shielding, structural, physical, and optical properties for a series of borosilicate glass. *Journal of Non-Crystalline Solids*, 550(August), 120360. <https://doi.org/10.1016/j.jnoncrysol.2020.120360>
- Mostafa, A. M. A., Elbashir, B. O., Issa, S. A. M., Uosif, M. A. M., Ene, A., Algethami, M., Bawazeer, O., El Agammy, E. F., & Zakaly, H. M. H. (2022). Influence of combining Al<sub>2</sub>O<sub>3</sub>, La<sub>2</sub>O<sub>3</sub>, Gd<sub>2</sub>O<sub>3</sub>, and Dy<sub>2</sub>O<sub>3</sub> with barium borosilicate glass-ceramics: A case study of gamma radiation interaction parameters. *Journal of Materials Research and Technology*, 19, 1972–1981. <https://doi.org/10.1016/j.jmrt.2022.05.095>
- Okada, T., Saito, J. ichi, Namie, M., & Nishimura, F. (2025). Synthesis of dilute acid-soluble platinum compounds in molten KOH-B<sub>2</sub>O<sub>3</sub> medium. *Materials Today Communications*, 42(November 2024), 111244. <https://doi.org/10.1016/j.mtcomm.2024.111244>
- Othman, A. M., Abd El-Fattah, Z. M., Farouk, M., Moneep, A. M., & Hassan, M. A. (2021). Optical spectroscopy of chromium doped bismuth-lithium borate glasses. *Journal of Non-Crystalline Solids*, 558(February), 120665. <https://doi.org/10.1016/j.jnoncrysol.2021.120665>
- Şakar, E., Özpolat, Ö. F., Alım, B., Sayyed, M. I., & Kurudirek, M. (2020). Phy-X / PSD: Development of a user friendly online software for calculation of parameters relevant to radiation shielding and dosimetry. *Radiation Physics and Chemistry*, 166, 108496. <https://doi.org/10.1016/j.radphyschem.2019.108496>
- Sayyed, M. I., Tekin, H. O., Kılıcoglu, O., Agar, O., & Zaid, M. H. M. (2018). Shielding features of concrete types containing sepiolite mineral: Comprehensive study on experimental, XCOM and MCNPX results. *Results in Physics*, 11(August), 40–45. <https://doi.org/10.1016/j.rinp.2018.08.029>
- Stone, H. B., Coleman, C. N., Anscher, M. S., & McBride, W. H. (2003). Effects of radiation on normal tissue: Consequences and mechanisms. *Lancet Oncology*, 4(9), 529–536. [https://doi.org/10.1016/S1470-2045\(03\)01191-4](https://doi.org/10.1016/S1470-2045(03)01191-4)
- Ummah, M. S. (2019). evaluation of radiation shielding integrity of fabricated concrete with some selected aggregate sizes. *fudma journal of science*, 11(1), 1–14. <https://fjs.fudutsinma.edu.ng/index.php/fjs/article/view/1525/1188>
- Yonphan, S., Limkitjaroenporn, P., Borisut, P., Kothan, S., Wongdamnern, N., Alhuthali, A. M. S., Sayyed, M. I., & Kaewkhao, J. (2021). The photon interactions and build-up factor for gadolinium sodium borate glass: Theoretical and experimental approaches. *Radiation Physics and Chemistry*, 188(January), 109561. <https://doi.org/10.1016/j.radphyschem.2021.109561>



©2025 This is an Open Access article distributed under the terms of the Creative Commons Attribution 4.0 International license viewed via <https://creativecommons.org/licenses/by/4.0/> which permits unrestricted use, distribution, and reproduction in any medium, provided the original work is cited appropriately.